Geologia Croatica
Journal of the Croatian Geological Survey and the Croatian Geological Society
2025 | 78/1 | 31–44 | 8 Figs. | 1 Suppl. | www.geologia-croatica.hr

Epikarst of the Eastern part of Suva planina Mt.: a new perspective defined from an integrated survey

Branislav Petrović[1]*, Snežana Ignjatović[1], Živojin Smiljković[2], Veljko Marinović[1], Violeta Gajić[1]

[1] University of Belgrade, Faculty of Mining and Geology, Đušina 7, 11000 Belgrade, Serbia; (*corresponding author: branislav.petrovic@rgf.bg.ac.rs)
[2] Serbian Environmental Protection Agency, Žabljačka 10A, 11000 Belgrade, Serbia

doi: 10.4154/gc.2025.03

Article history:
Manuscript received: July 26, 2024
Revised manuscript accepted: November 05, 2024
Available online: January 30, 2025

Keywords: epikarst, applied research, karstification, Suva planina Mt., SE Serbia

Abstract

Human interest in karst groundwater stems from the high-quality water that karst aquifers can accumulate. In Europe, 21.6% of the land is covered by carbonate rocks, with Serbia having 10.3% karst coverage. Understanding karst aquifers is essential for sustainable water management. The epikarst layer has higher water permeability and diffuse circulation. This study focuses on the Suva planina Mt. karst aquifer system and its "first" layer – epikarst. During the survey, an innovative methodology was employed, combining indirect methods like remote sensing with field techniques such as geomorphological research, hydrogeological and epikarst mapping, geophysical surveys, petrological/sedimentological research, and pedological studies. This combined approach yielded exceptionally good results. Using satellite imagery (remote sensing) helped define the general groundwater flow and the distribution of epikarst on the eastern slopes of Suva planina Mt. The epikarst potential (E) map created, guided further detailed field mapping, improving the understanding of the area's geology and geomorphology, and identified locations for geophysical surveys and sampling. Field geomorphological research refined the distribution and characteristics of the epikarst, with hydrogeological mapping on benchmark profiles providing on-site data. Four categories of epikarst were identified. Geophysical surveys using vertical electrical sounding offered insights into fractured and karstified zones up to 30-100 metres deep. Petrological research identified limestone types, while pedological analyses defined soil types and geochemical properties, highlighting the soil and epikarst's role in altering infiltrating water quality. Continued multidisciplinary research on Suva planina Mt. is essential for understanding groundwater systems. Enhanced geophysical methods and pre-field drone surveys are recommended for future studies, along with increased soil sampling from areas of diverse vegetation.

1. INTRODUCTION

Human interest in karst groundwater has been impacted by the huge amount of good quality water that karst aquifers can accumulate and yield. About 21.6% of the European land surface is covered by carbonate rocks, with a total area of actual carbonate rock outcrops of 13.8% of the total European surface. Similar coverage of the surface, with limestone of the Mesozoic period, occurs in Serbia with open karst over 10.3% of the area (CHEN et al., 2017). Therefore, it is necessary and crucial, to become familiar with karst aquifer characteristics to manage it sustainably.

In karst areas, the upper layer of epikarst could play a crucial role in protecting karstic formations. Epikarst represents the highest part of the rock mass exposed to karstification, i.e. a layer of partially altered bedrock that has not yet developed into soil. In this layer, water permeability (due to cracking) and the diffuse circulation of water are significantly higher and more evenly distributed both vertically and horizontally compared to the rest of the karstified rock mass (KLIMCHOUK, 2000). In most karst regions and formations, the presence of an epikarst zone is expected. The thickness of the epikarst zone can vary widely, from 10 cm to 30 m, typically estimated to be several metres up to 10-15 metres (KLIMCHOUK, 2000, 2004).

There are many specific methods for researching the karst (epikarst) such as (PETROVIĆ, 2020a; STEVANOVIĆ, 2015; GOLDSCHEIDER & DREW, 2007): speleology, karst hydrology/hydrogeology, karstology, speleobiology, cave diving (speleodiving), etc.

Here, we present integrated methods for surveying karst (specifically epikarst), which include remote sensing, geomorphological research, geophysics survey, hydrogeology and epikarst mapping, petrology/sedimentological research, and a pedological survey. These integrated methods were used to define the epikarst of the Eastern part of Suva planina Mt. and to explore the formation and function of this specific layer in the aforementioned setting.

2. CHARACTERISTICS OF THE STUDY AREA

Suva planina Mt. is located approximately 230 km SE of Belgrade. The name of the mountain (Suva = Dry) originates from the fact that there are only a few springs on the higher slopes of the massif, and only two springs discharge almost all year round: Bojanine Vode (860 m a.s.l.) and Rakoš (1280 m a.s.l.). The karst aquifer system of Suva planina Mt. is formed

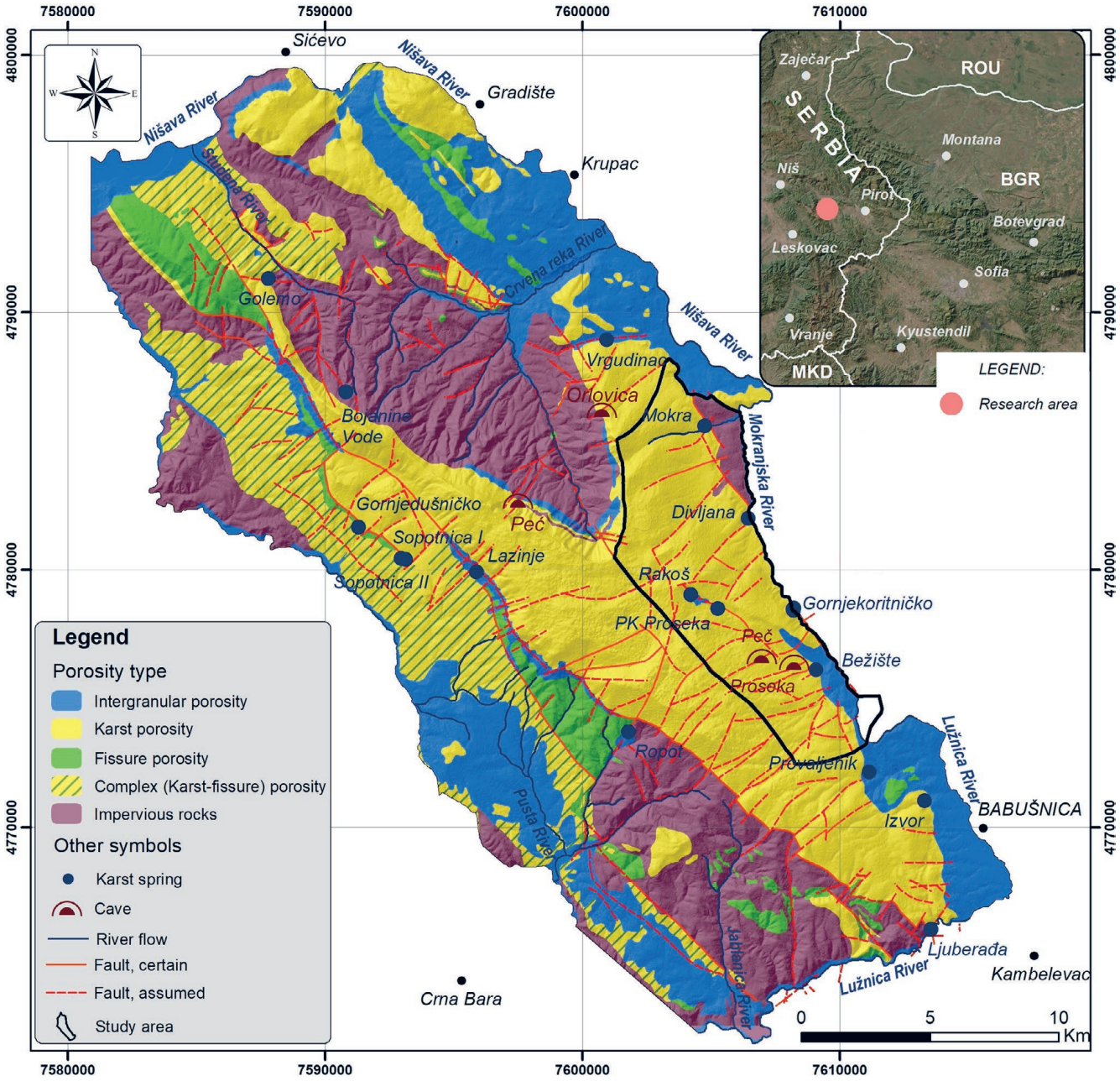

Figure 1. Location of the study area and hydrogeological map (adapted from PETROVIĆ, 2020b).

in the limestones of Middle and Upper Jurassic and Lower Cretaceous age on the north-eastern slopes of the mountain (PETROVIĆ, 2020a, b; MARINOVIĆ & PETROVIĆ, 2021; PETROVIĆ et al., 2023; PETROVIĆ & MARINOVIĆ, 2023). The local faults provoked the enhancement of the karstification process in the limestone and dolomite, and the groundwater flow has been directed transverse to the original NW-SE direction (STEVANOVIĆ, 1991; PETROVIĆ, 2020a, b). On Suva planina Mt., Peć cave in Barski Hrid and Orlovica cave in Ostrovica, north of the area that was the subject of detailed investigation works, as well as two small jamas (shafts): Jama in the Konjsko area and Ledenica in the Ždrebica area (on the western slope of Suva planina) were found (PETROVIĆ, 1976). Underground karst formations are present on the eastern slopes of Suva planina Mt., but are dissimilar to those on the northern and western vertical limestone cliffs. The underground karst phenomena discovered in the research area are the Prosek jama and the Peč cave, in the area of the village of Bežište (Bukovica area) (PETROVIĆ, 2020a; PETROVIĆ, 2023).

Additional karstification provided further and finer division of the groundwater flow and resulted in quite a few orifices of the aquifers in the foothills of Suva planina Mt. (PETROVIĆ & MARINOVIĆ, 2021; PETROVIĆ et al., 2023). Karst springs that originate from the carbonate rocks of Suva Planina Mt. (Fig. 1) and are used for the public water supply include: Mokra, Divljana, Gornjekoritničko, Bežište, Ljuberađa, Lazinje, Sopotnica I and Sopotnica II, Gornjedušničko and Golemo. However, the Bojanine Vode, Vrgudinac, Ropot, Provaljenik, Izvor, PK Proseka, and Rakoš springs have also been used for water supply, but their quantity and sometimes the quality are not always adequate. During the 1980's, a few of the karst springs were captured for a water supply to Niš city: Mokra ($Q_{avg} \approx 550$ l/s), Divljana ($Q_{avg} \approx 450$ l/s), Ljuberađa

(Q_{avg} ≈ 850 l/s), and Golemo (Q_{avg} ≈ 300 l/s), while Gornjedušničko (Q_{avg} ≈ 200 l/s) has been captured for a water supply to the town of Gadžin Han. The recharge of aquifers is precipitation based with effective infiltration estimated up to 350 mm (STEVANOVIĆ, 1991, 1994; PETROVIĆ, 2020b).

The research area has a moderate-continental climate with characteristically long and cold winters and relatively warm summers. The average annual precipitation for the period 1991–2018 is 593.8 mm (according to data from the Republic Hydrometeorological Institute of Serbia, analysed in PETROVIĆ, 2020b). The average multi-year air temperature for the same period is +12.6 °C.

3. METHODOLOGY

During the study, an innovative methodology of a combination of indirect survey methods (remote sensing) together with field survey (geomorphology research, hydrogeology and epikarst mapping, geophysics survey, petrology/sedimentology research and pedology research) was used, indicating that the combination gives extremely good results. Field surveys and sampling have been conducted in several localities within the research area: Rakoš spring, Bukovica (area between Peč cave and Bežište), Bežište village, Mokra village and Divljana village (Figs. 2 and 3).

The application of remote sensing of satellite images (Landsat 8 image courtesy of the U.S. Geological Survey) and analysis of the rupture structure of the terrain taken from the Basic Geological Map (BGM) of SFR Yugoslavia, sheet Bela Palanka VUJISIĆ et al. (1971), served to define the presence of ruptures and as a basic preparation for field research of the epikarst. The interpretation of Landsat 8 was performed with a channel 5, 6 and 7 combination (WON-IN & CHARUSIRI, 2003), as well as with a channel 7, 6 and 2 combination (GISGEOGRAPHY, 2024). The raster files were filtered with an image enhancement tool to improve the quality. Contrast enhancement of "raw" images was performed by selective linear transformation of the original pixel values. The colour-composite images allowed for easier observation of linear elements and the creation of a map of the rupture assembly, with the use of the convolution function in filtering the images (ARCGIS, 2024). Also, spatial filtering of recordings was performed using the process of highlighting line elements with an edge enhancement tool to improve the perceptibility of ruptures. Remote detection was also applied during vegetation analysis (AGRICOLUS, 2024), by determining the normalized difference vegetation index – NDVI, as well as by defining the normalized moisture deficit index – NDMI. As part of the epikarst research, analysis of the geomorphological characteristics of the terrain was performed (e.g. of the topography of the terrain, and of the digital elevation model – DEM 10 m resolution). Furthermore, analysis of the geological composition was performed from the aspect of rock susceptibility to karstification as well as analysis of soil and vegetation as factors influencing the epikarst (PETROVIĆ, 2020b; PETROVIĆ et al., 2022). These analyses resulted in the creation of layers (N – vegetation NDVI; P – soil protection; S – slope; K – degree of karstification) that were used for designing the Map of potential for epikarst development – E map. The map of potential for epikarst development was created according to the formula: E=2N+P+2S+3K (PETROVIĆ, 2020b; PETROVIĆ et al., 2022). The final map has four categories of potential for epikarst development: 1 – low, 2 – medium, 3 – high and 4 – very high.

Geomorphological research was carried out in several stages, during which the existence, number, arrangement and size of large geomorphological objects such as sinkholes, uvalas, jamas and caves within the research area were determined. The recording of the coordinates of phenomena and objects on the ground was carried out using the Global Positioning System (GPS), while the dimensions of the objects were determined using a laser range finder (Leica Disto Lite 5).

Geophysical surveys were undertaken using the electrical method, applying the technique of vertical electrical sounding (VES). The VES technique gives good results when examining horizontal or sub-horizontal layers (REYNOLDS, 2011). The karst receives more water in the case of zones with higher resistivity, while it receives less water in the case of zones with lower resistivity. Zones with low resistivity are more karstified, while zones with high resistivity are less karstified (VERESS et al., 2023). Karst phenomena can be predominantly air-filled and then have high resistivity (e.g., >1000 Ωm) or partly or totally water-filled with resistivity between 60 Ωm to 1000 Ωm. Depending on the ionic concentration of the groundwater in the karst structures (features), which are partly or totally water-filled, they may have resistivity values varying from low (e.g., 60-100 Ωm) to relatively high (e.g., 100-250 Ωm), in comparison to the host rock (e.g., >2000 Ωm for non-karst limestone) (TORRESE, 2020). The VES technique is applied to determine the change of electrical resistivity with depth using the Schlumberger array. The Schlumberger array is mostly used in vertical electrical sounding for its better depth penetration. In this array, four electrodes are placed in a line around a common midpoint. The two outer electrodes (A and B) are current electrodes, and the two inner electrodes (M and N), are potential electrodes placed close together. To obtain the maximum depth penetration in the VES procedure, the distance between the potential electrodes does not change and the current electrodes are moved away, thus increasing the depth penetration. As a result of the application of this technique, electrical sounding diagrams were obtained. These diagrams are displayed using a bi-logarithmic diagram where the electrical resistivity is given as a function of the half-distance of the current electrodes (AB/2). During the survey, the distance between the current electrodes (AB/2) ranged from 30 m to 300 m.

The rock samples, marked RS1 to RS7, taken during field investigations within the research area were subjected to petrological analysis. Of the seven rock samples, three were taken from the Peč cave and its immediate surroundings, while four others were taken from specific locations within the research area (Figs. 2b and 3). The rock samples were taken from the surface of the terrain, except for sample RS2 that is taken from the interior of the cave. Sample RS1 is from the surface above the cave Peč and sample RS3 was taken about 100 metres from the entrance of the cave. Two samples RS4 and RS5 were taken from the surface of the terrain between the Peč cave and Bežište karst spring – Bukovica area (Fig. 2b) and one sample RS6 was from the exposed limestone

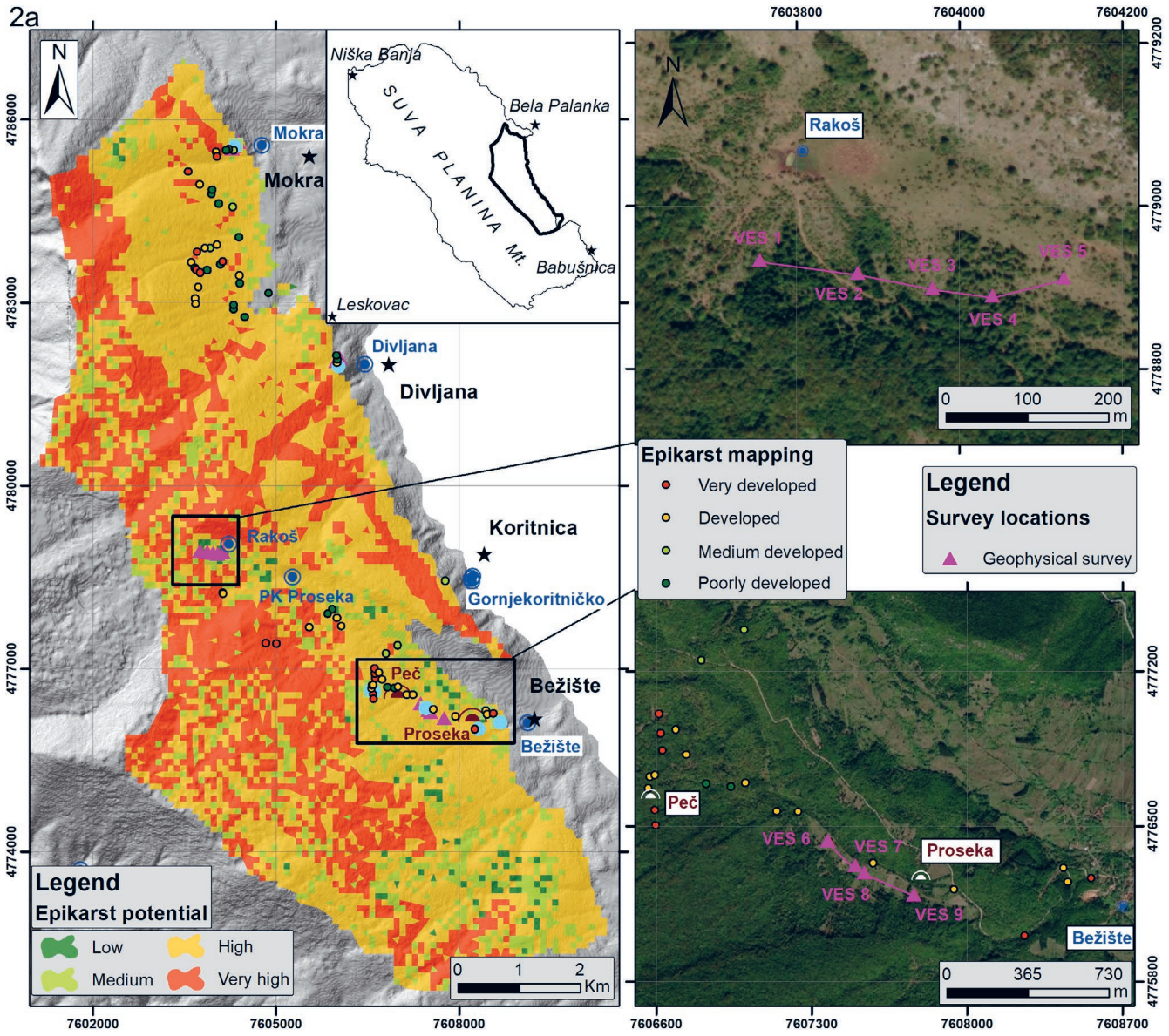

Figure 2. a) The E map of the area with locations of the geophysical field surveys: Rakoš spring (up) and Bukovica area (down). **b)** The E map of the Bukovica area and Bežište karst spring area with sampling locations of soil (up) and rocks (down).

above the Bežište karst spring. The sample RS7 represents a limestone rock from the immediate surroundings of the Mokra spring and its hinterland (Fig. 3). During macroscopic examination, the samples were tested with diluted hydrochloric acid (HCl). To determine the calcite content in these carbonate rocks and apply the appropriate classification, a quick method for determining the $CaCO_3$ content in the rock – calcimetry – was applied. The mineral composition of the studied sedimentary rocks was determined by examining the petrographic preparations on a polarizing Zeiss microscope for transmitted light coupled with a Zeiss Axiocam 208 colour digital camera. Examinations of petrographic samples of sedimentary rocks included the determination of structure and grain orientation, as well as some of the textural characteristics. All analysed samples of limestone were first defined optically, which determined the direction of further study. Micropaleontological examinations were carried out via examination of thin-sections (transparent petrographic/micropaleontological preparations). Analyses were performed using an Olympus brand polarizing microscope (type BH50). Micropaleontological analysis of thin-sections included the determination of foraminifera and other microfossil content.

Within the framework of land cover (soil) research, parameters of soil samples (S1-S8) were determined in the laboratory: soil moisture, mineral composition, soil organic matter content, as well as the physico-chemical processes that occur within it, influencing the changing properties of surface (ground) waters. The soil samples were taken from the following locations: S1 – from the interior of the Peč cave, sample S2 was taken about 100-150 metres from the entrance to the cave (Fig. 2b). Two samples (S3 and S4) were taken in the Bukovica area between the Peč cave and the Bežište karst spring (Fig. 2b) and one sample S5 was from immediate vicinity of the Bežište karst spring. Sample S6 was taken between the villages of Gornja Koritnica and Divljana (Fig. 3). Samples S7 and S8 represent a soil from the immediate surroundings of the Divljana karst spring and the Mokra

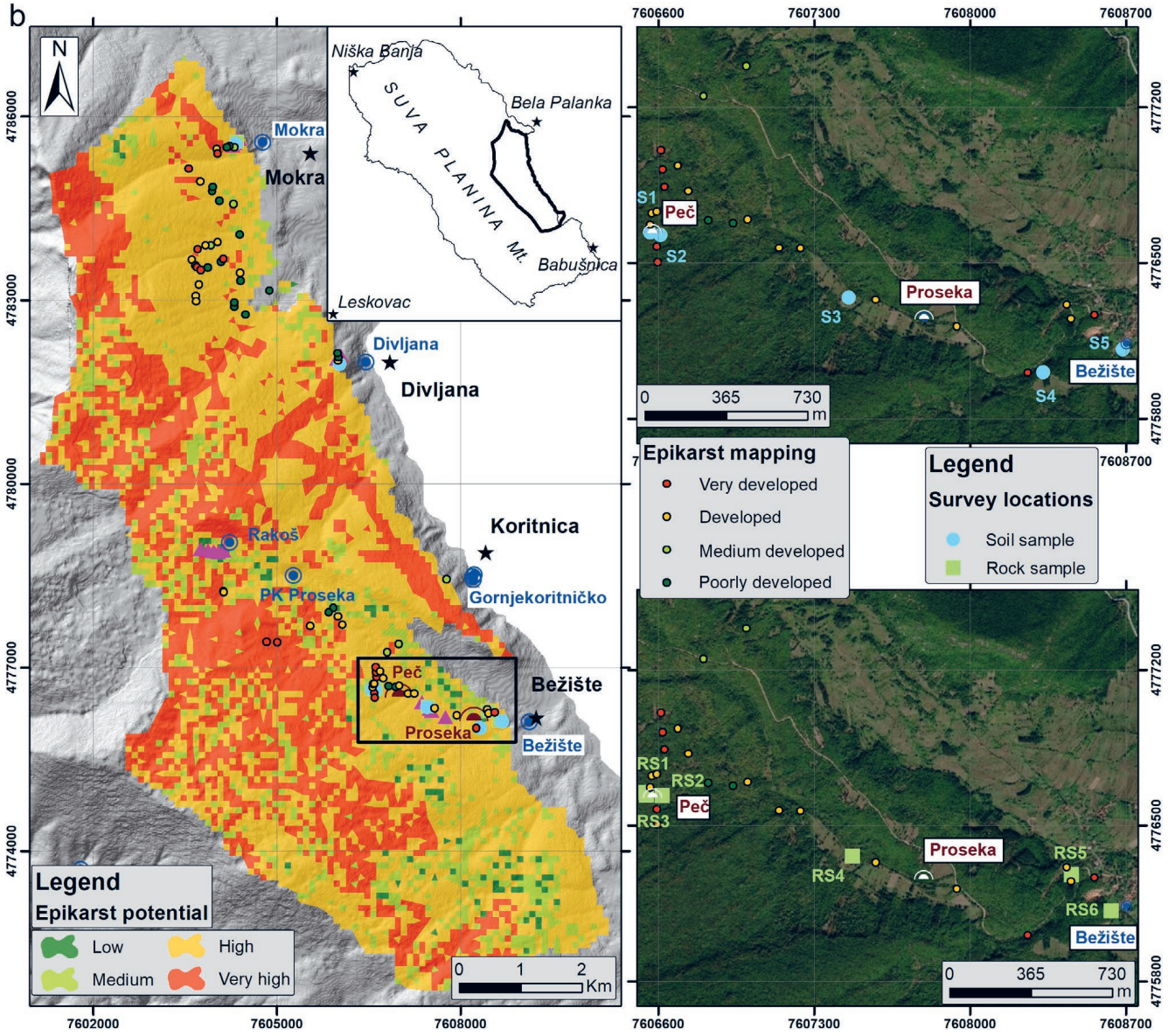

Figure 2. continued.

spring, respectively (Fig. 3). In addition, the objectives of the physico-chemical compositional research of the soil were to:

– Perform technical analysis of samples and determine the amount of organic matter present
– Determine whether the soil is contaminated with any heavy metals.

The determination of the content of all major and trace elements that make up the soil was carried out at the Laboratories of the Faculty of Chemistry, University of Belgrade. Standards SRPS B.H8.390/1987 and ISO 1171 were used for the preparation of samples for technical analysis (moisture and ash content) (SMILJKOVIĆ, 2019; PETROVIĆ, 2020b). Elemental analysis determined the content of hydrogen, nitrogen, sulphur, and organic carbon. Organic carbon was analysed after the removal of carbonates with diluted hydrochloric acid (1:3 v/v). Measurements were carried out on the Vario EL III, CHNOS Elemental Analyzer, GmbH apparatus. Sample preparation for the analysis of macro- and microelements in soil was performed using microwave digestion (ETHOS1-Advanced Microwave Digestion Milestone). The content of macro- and microelements was determined by optical emission spectrometry with inductively coupled plasma (ICP-OES) on a Thermo Scientific Cap 6500 Duo ICP instrument (Thermo Fisher Scientific, Cambridge, UK). Standards for the preparation of the standard series were used during this process (Multi-Element Plasma Standard Solution 4, Specpure®; Silicon, plasma standard solution, Specpure®, Si 1000 µg/ml; SS-Low Level Elements ICV Stock 10 mg/l: Ag, Al, As, Ba, Be, Cd, Co, Cr, Cu, Mn, Mo, Ni, Pb, Sb, Se, Th, Tl, U, V, Zn).

Hydrogeological and epikarst mapping was carried out in parallel with the geomorphological research, after geophysical surveys. The mapping included defining the characteristics of the epikarst on open rock outcrops and cuts, where the thickness of the epikarst, its composition and area of distribution were determined, and data collected were prepared for correlation with facts already collected by remote sensing and with details presented on the Map of potential for epikarst development (PETROVIĆ, 2020b; PETROVIĆ et al., 2022).

4. RESULTS AND DISCUSSION

Remote sensing was used during the analysis and extraction of lineaments on the processed (RGB) combination raster 567 and 762, as well as when defining the NDVI and NDMI, which together helped in the formation of the Map of potential epikarst development (Fig. 2). The potential for epikarst development depends firstly on existing tectonic conditions (faults and cracks) and the increased influence of vegetation. The influence of the forest vegetation is through the work of the root system, the retention of other living things in the surface litter created from fallen leaves, and the increase of carbon dioxide content due to the unfolding of life processes and the process of decomposition of organic matter, as well as other chemical compounds that have a corrosive effect on the limestone in the basement. The E-map has 4 categories (Figs. 2 and 3; 1 pixel=100 m): 1 – low potential, 2 – medium potential, 3 – high potential, and 4 – very high potential. Surfaces of different potential categories for epikarst development are shown in four colours from green (Low potential) to red (Very high potential). In the E map the area of the terrain that shows a low potential for the development of epikarst occupies only 1.5% of the area of exposed carbonate rocks in the research area, while the medium potential for the formation of epikarst represents 11.5% of the area. 53% of the exposed limestone area has a high potential for the formation and development of epikarst, and 34% is very high (PETROVIĆ, 2020b; PETROVIĆ et al., 2022).

Considering the size of the pixels it should be emphasized that the E map cannot be used independently to define the degree of real development of the epikarst, without further field research. Therefore, the next step in the research was the mapping of the epikarst on open outcrops and cuts (Fig. 4, a-d), when the thickness of the epikarst, its composition and area of distribution were determined. For the purposes of defining the degree of karstification and epikarst evolution in the research area of the Suva planina Mt. four categories of this subsurface layer were distinguished (Fig. 4, 1-4). Categories were made primarily according to the thickness of the zone, then according to the thickness of the soil layer located on the surface and finally the presence and type of vegetation.

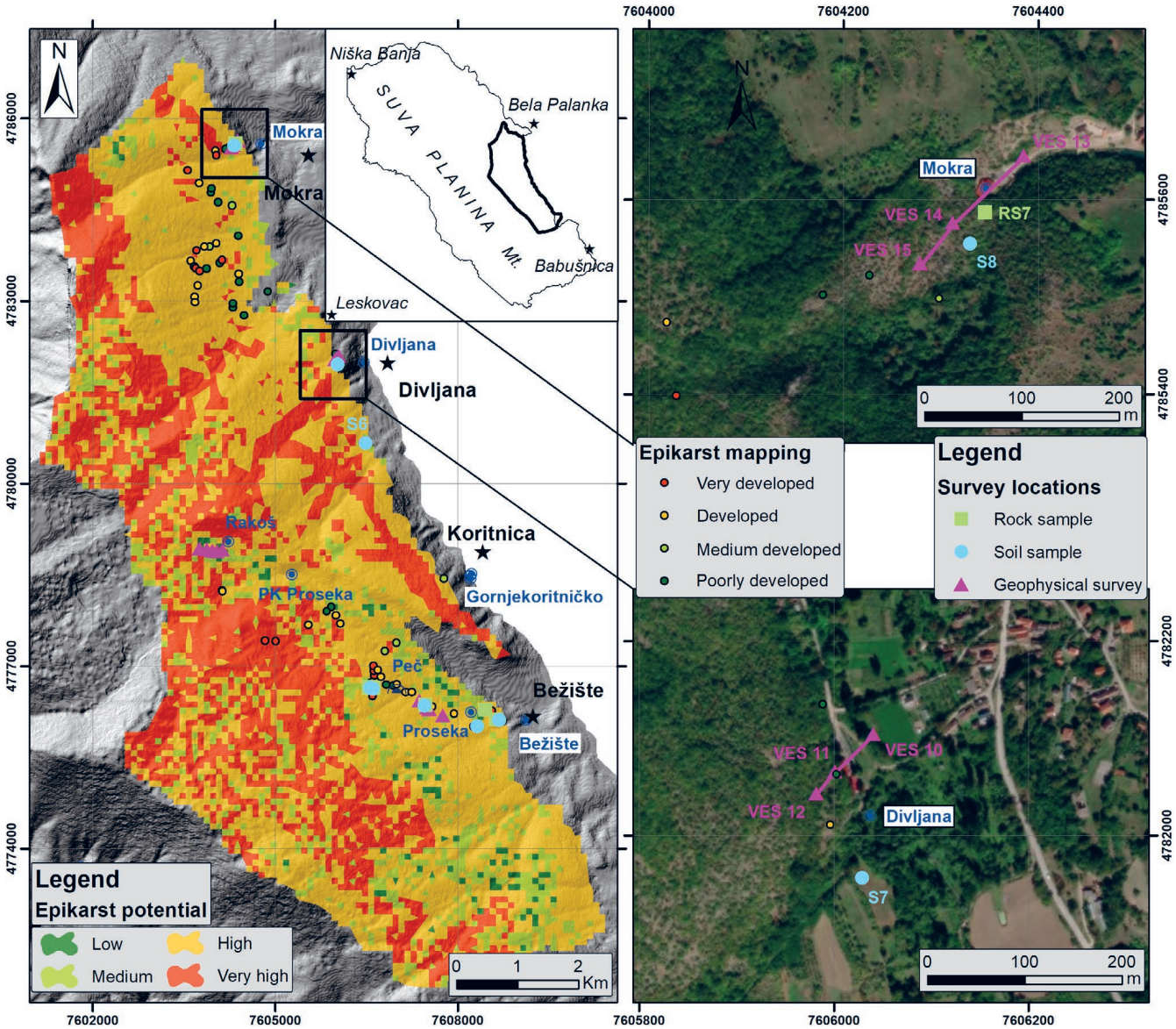

Figure 3. The E map of the area with locations of geophysical field surveys, rock and soil sampling around Mokra (up) and Divljana (down) karst springs.

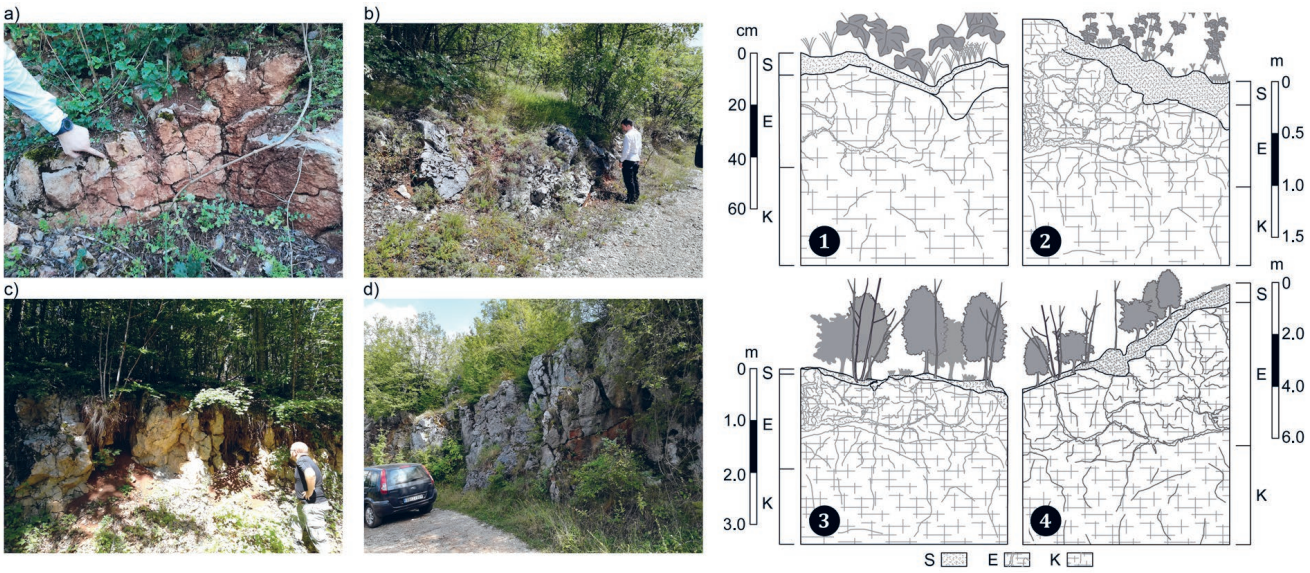

Figure 4. The mapping of the epikarst on open outcrops and cuts with degree of epikarst development: Mapping of the epikarst on open outcrops and cuts – **a), b), c)** and **d)**. Epikarst categories: **1**, **2**, **3**, **4**; Legend: S – soil, E – epikarst, K – karst.

The first category (Fig. 4-1) is poorly developed epikarst up to 50 cm thick, sometimes up to 1 m, on which the presence of cracks filled with soil can be observed, the thickness of the soil layer is up to 10 cm, when it is present. The second category (Fig. 4-2) is developed epikarst characterized by the presence of a significantly thicker layer of soil on the surface of 10 to 30 cm (rarely up to 50 cm), while the epikarst layer is about 1-1.5 metres thick, wider cracks and caverns (centimetre dimensions) can be observed, and which are often not fulfilled. The third category (Fig. 4-3) is medium-developed epikarst characterized by a significant thickness of the base layer, up to 3 metres, but it is most often 1.5 to 2 metres thick, the soil is of varying thickness from 10 to 30 cm, it can also be absent on smaller areas (the epikarst is bare), cracks and channels are common, and are often filled with secondary material. The fourth category (Fig. 4-4) is extremely well developed epikarst that has all the characteristics of the previous category, only the thickness of the epikarst is always over 3 metres. Categories separated and created with the help of remote sensing methods coincide with mapping and field research to a lesser degree than expected. The inconsistency of the results obtained using remote sensing and field surveys exists for several reasons. Primarily, the pixel size on the map (100 px) is larger than necessary for this level of research, because the local epikarst and its degree of development can change at distances of less than 50 m. It is necessary to have more detailed geological mapping than the 1:25 000 maps used here.

The thickness of the epikarst in the survey area was defined by the VES technique as well. Measurements using the VES technique were done on locations that have been chosen based on geomorphological and hydrogeological surveys. The VES was done on locations Rakoš, Bukovica, Divljana and Mokra. In the Rakoš area (Fig. 2a), the distance between the current electrodes (AB/2) was 30 m. In the Bukovica area the distance between the current electrodes (AB/2) was 30 m and 110 m (Fig. 2b). The distance between the current electrodes (AB/2) in Mokra and Divljana locations was 50 m to 300 m (Fig. 3).

The VES measurements on Rakoš were done along profiles VES1–VES5 (Fig. 2a). The results in points VES1, VES2 and VES3 show that the measurement is done in the fault zone (Fig. 5a). This zone is without a diluvial overlay with high values of specific electrical resistivity from the surface to a depth of over 2 m. The measurement points VES1 and VES2 are located over the fault zone on a relatively raised block with a diluvial layer and debris material in it. The measurement points VES4 and VES5 are located on the raised flank of the fault and VES5 is located the farthest from the fault zone. The data from VES5 show that diluvium and clay are found in this part, which are washed closer to the fault and eroded onto the flank that descends. The results of VES measurements at the Rakoš indicate that there are zones of lower and higher resistivity. In the shallowest part of the terrain, the resistivity is high indicating that this part of the terrain contains limestone rubble in a dried clay matrix. The change by the depth of high and low resistivity (VES1–VES4) is related to the change of dry larger limestone blocks and degraded limestone belts with water, or clay as a filling. The VES5 measurements show that such heterogeneity of the limestone is not visible, but beneath the clay layer lies weakly cracked limestone, to a depth of almost 20 m. The results of a geophysical survey on Rakoš along the profile VES1–VES5 (Fig. 5a) shows the layer consisting of decomposed and altered limestone rock material (breccia and debris) and soil, which in this case represents the epikarst. The thickness of the epikarst at the Rakoš ranges from 3 to 15 metres.

At the Bukovica location, the VES measurements were undertaken along profiles VES6–VES9 (Fig. 2a). The results in points VES6, VES7, VES8 and VES9 show that the measurement is also undertaken in the fault zone (Fig. 5b). The results along the profile VES6–VES9 indicate that the resistivity increases with depth and that there is a dry system of cracks, pits and caverns below the surface. The results of

VES on the Bukovica profile show the layer consisting of decomposed and altered limestone rock material (breccia) and soil, which in this case represents the epikarst. The thickness of the epikarst at the Bukovica ranges from 1.5 to 9 metres (Fig. 5b). In this area, the epikarst overlies a well karstified limestone in which there is a system of dry cracks, caverns, and larger channels.

At the Mokra location, the VES measurements were made at three points VES10, VES11 and VES12 (Fig. 3). This research indicated that the base of the karstification is located at >95 m depth. The results of VES at point VES10 show that there is dry karstification beneath the examined terrain (Fig. 5c). The measurement point VES11 is located exactly above the karst spring and the results of the measurements indicate that there is cracked limestone below. At the level of the karst spring, at a depth of about 15 m, the influence of groundwater appears. The thickness of the epikarst at the Mokra site ranges from 0.5 to 4 metres.

Finally, at the Divljana location, the VES measurements were undertaken at three points VES13–VES15 (Fig. 3). This research established that the base of the karstification depth in this area is around 100 m. The results of VES at point VES13 show that there is dry karstification below the examined terrain (Fig. 5d). The measurement point VES14 is located above the karst spring and the results of the measurements indicate that there is fissured limestone with groundwater. The thickness of the epikarst at the Divljana site ranges from 0.5 to 4 metres.

The examined samples of limestone are dark grey in colour and have a crystalline structure. The rock surfaces are often covered with white calcite scrums (up to 3 mm thick) and powdery limonite (rust colour). Limestones are strongly tectonized, which was manifested by the appearance of white calcite cracks/wires. The sample from the Bežište area (RS5) underwent strong recrystallization (Fig. 2b). They are very hard and compact, breaking into pieces with rough fracture surfaces and sharp fracture edges. Considering the textural features, we can note that oscillogram-type stylolitic seams marked by dark, non-carbonate minerals (ingredients) stand out.

Macroscopically, allochemical components can be observed. Usually, the allochemical component is relatively fine-grained, consisting of peloids and organic residues, with sections of macrofossils, with uniform dimensions of 2 to 5 mm in most of the samples. In addition, sections of circular, ellipsoidal shapes up to 1 cm in size could be noticed in some samples (Fig. 6). Structurally, the rocks correspond to FLUGEL (2004): Wackestone (RS1, RS4 and RS5) and Packstone (RS2, RS6, RS7) microfacies and Grainstone (RS3). Irregular dissolution structures are also developed in some rocks; fenestrae, that are filled with crystalline calcite (geopetal structure). Cracks and microcracks filled with coarse-grained neocalcite are also present. Bioclasts are represented by an association of marine microorganisms and their content is 20-25%.

According to the content of allochems and orthochems (FOLK, 1959), the investigated sample RS1 corresponds to biopelmicrite, RS2 corresponds to pelbiosparite, RS3 corresponds to biointrasparite/biopelsparite, RS4 and RS5 corresponds to biomicrite, RS6 corresponds to biointramicrosparite and RS7 corresponds to fossiliferous micrite/biomicrite.

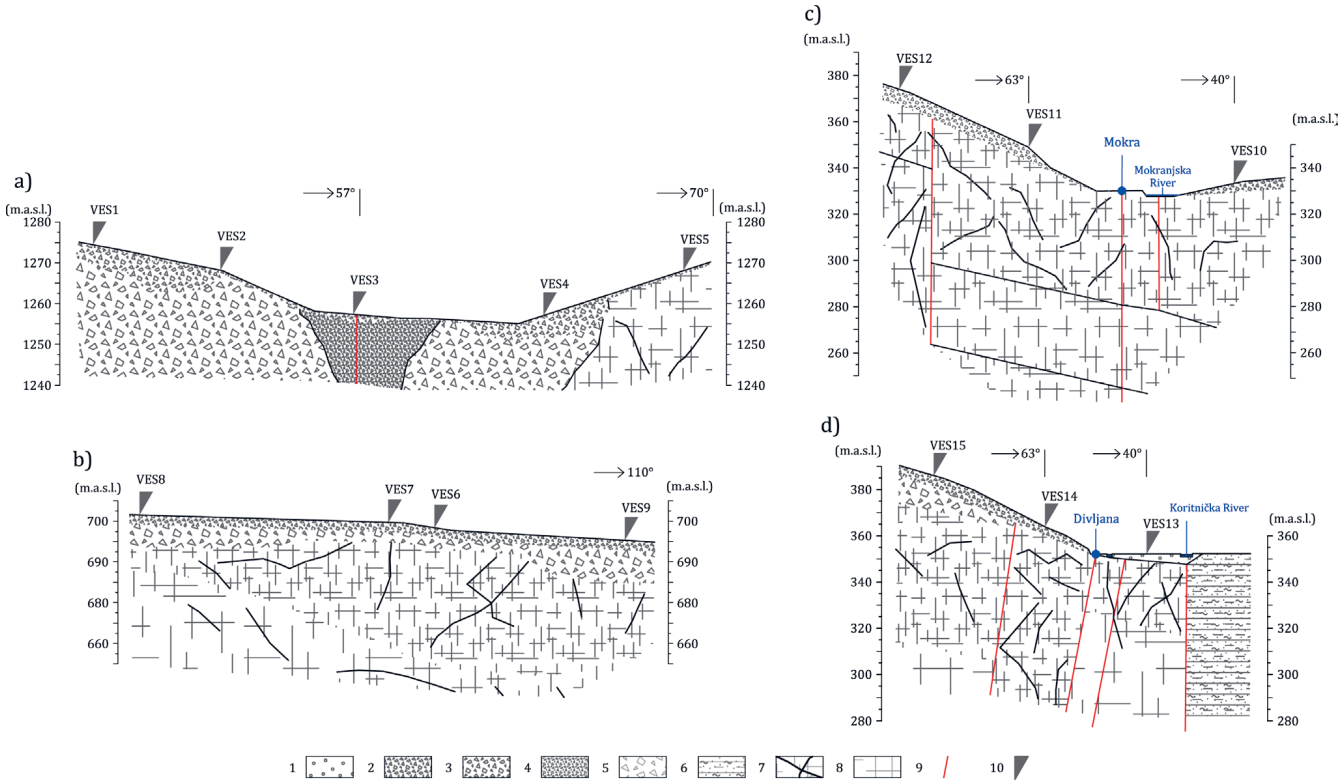

Figure 5. The interpretation of the VES measurements at selected locations: **a)** Rakoš spring area, **b)** Bukovica area, **c)** Mokra karst spring area, **d)** Divljana karst spring area. Legend: **1** – alluvium; **2** – colluvium with clay infill; **3** – breccia; **4** – resedimented breccias (fault area); **5** – breccia (limestone); **6** – sands, marls, gravels, clays; **7** – highly karstified limestone; **8** – limestone; **9** – fault; **10** – VES location.

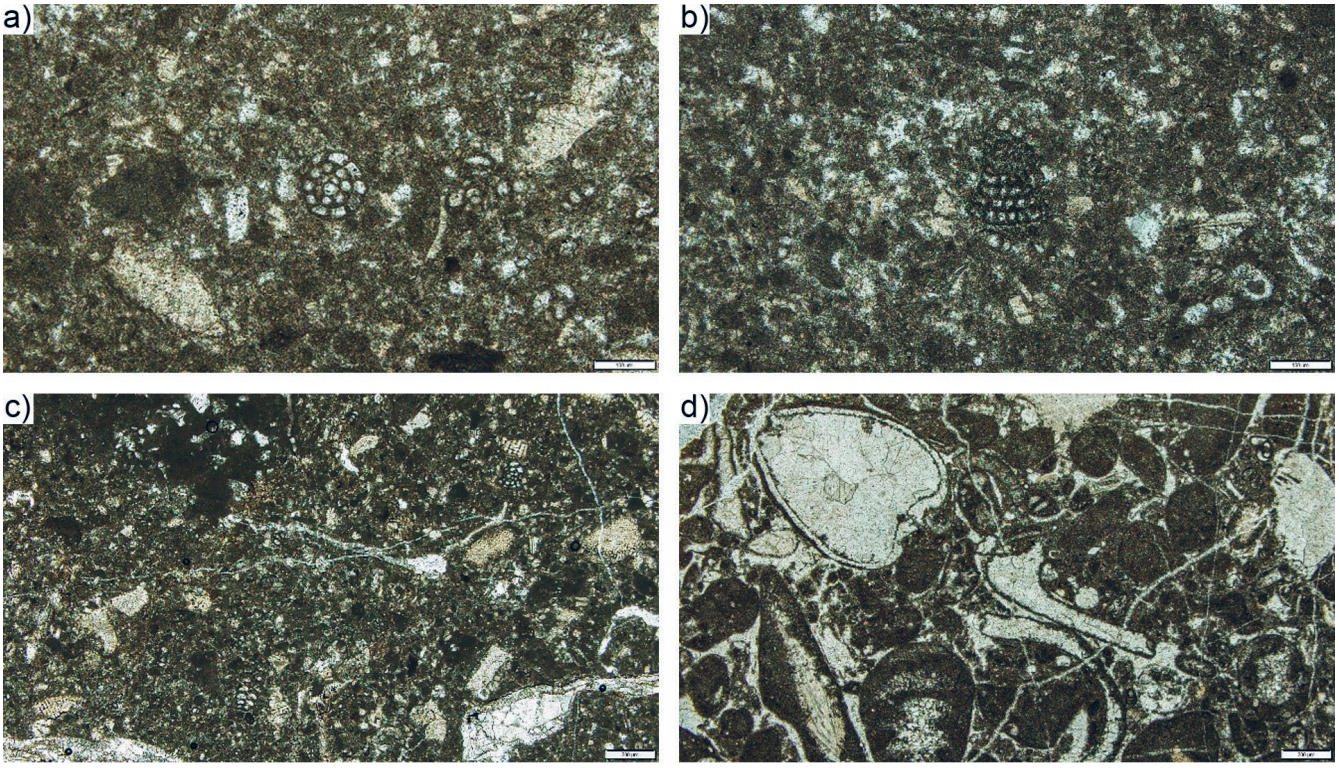

Figure 6. Some of the microfossils determined during the research: **a)** Sample RS4 in the centre *Debarina* cf. *hahounerensis;* **b)** RS5 – in the centre *Vercorsella* sp. **c)** RS5 – association of *Novalesia* sp., *Debarina* cf. *hahounerensis* and fossils of a shallow sea; **d)** Sample RS6 – microfossils of a shallow sea – *Pseudocyclammina* sp., Bivalvia and other micromolluscs.

Limestones are characterized by an association of benthic foraminifera microfauna, with a low diversity of forms, and the detritus of shallow marine fossils. Bioclasts could be represented by an association of marine microorganisms and their content is up to 25%. The chambers of foraminifera are filled with crystalline calcite. Some of the microfossils have been determined (Fig. 6): *Debarina* cf. *hahounerensis* FOURCADE, RAOULT & VILA, *Novalesia* sp., *Pseudocyclammina* sp., *Vercorsella* sp., *Nautiloculina* sp.

The sedimentological interpretation based on the analysis of the available investigated limestones of Suva planina Mt. shows that they were created in a marine environment of the very shallow subtidal and slightly deeper intertidal zones. The origin of these limestones is most probably related to the outer edge of the carbonate platform, with low water energy, with a transition to less protected parts of the platform (lagoon). Based on the biostratigraphic considerations of the entire determined association of foraminifera, the studied limestones correspond to the Upper Jurassic (RS2) and Lower Cretaceous periods and are related to shallow to slightly deeper subtidal depositional environments.

Considering that the calcite content in the samples RS1 and RS2 exceeds 97%, it is not surprising that the karstification and the formation of channels and caverns of metre dimensions are very pronounced. It can also be concluded that the composition of the rocks on the eastern slope of Suva planina Mt. favours the emergence of the karstification process and its rapid progress, especially in combination with the tectonic movements that caused the rise of the anticline and cracking of the limestone layers, thus the emergence of epikarst on this terrain is not in question. The somewhat lower percentage of calcite in some samples was also reflected in the degree of karstification within the Cretaceous rocks, which make up part of the terrain hypsometrically lower than the Peč cave, as well as the terrain that forms a large part of the Mokra, Divljana, Gornja Koritnica and Bežište springs catchment area.

Pedological research was initiated as part of the mapping process when basic data on the presence and thickness of soil were collected. Samples for geochemical characterisation (S1-S9) were collected from specific locations on the eastern slopes of the Suva planina Mt. (Figs. 2b and 3). The technical analysis of 8 soil samples (S1-S8) and one rock sample of limestone (S9) were conducted (Fig. 7), determining the quantity of organic matter (organic pollutants), and specific organic-geochemical parameters (SMILJKOVIĆ, 2019; PETROVIĆ, 2020b). The level of contamination (Fig. 8) with heavy metals was defined according to Serbian legislation (OFFICIAL GAZETTE RS, 2018).

The moisture content in the soil samples ranges from 2.62% to 7.72%, while in the reference sediment – S9 it is only 0.10%, which may indicate the absence of hygroscopic components that retain moisture. This assumption is also confirmed by the result showing that the sediment is composed of 99.90% carbonates. The ash content ranges from 62.94% to 90.71% indicating that the soil is expected to be predominantly mineral. The sediment has the lowest ash content compared to other samples, 56.83%, which can be explained by the fact that during heating to over 800 °C, carbonates degrade into oxides with the release of CO_2. Carbonate content values range from 17.46% to 80.40%. A higher carbonate content is noticeable in

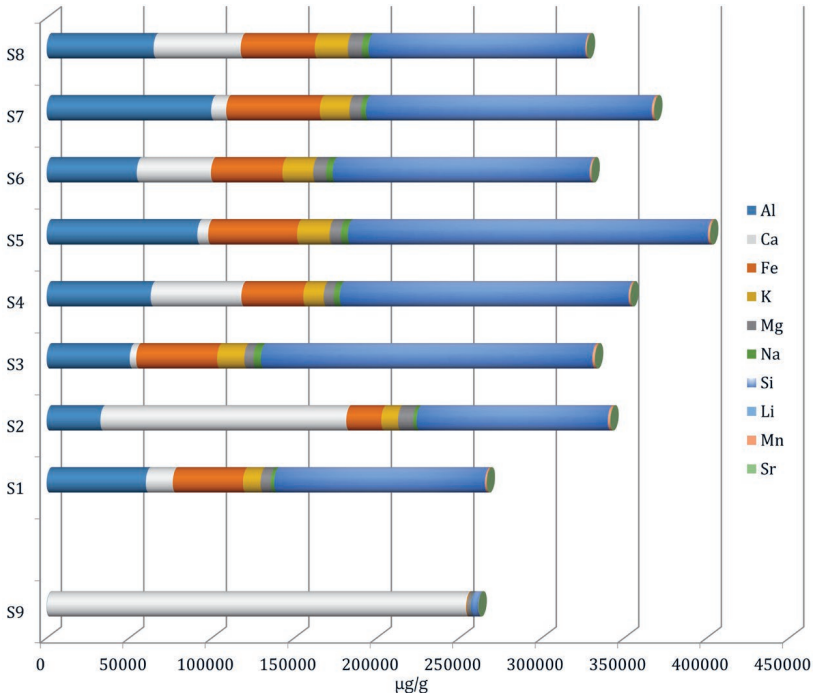

Figure 7. The macroelements in the soil (S1-S8) and rock (S9) samples.

samples S1-S4, especially in sample S2, which can be explained by the fact that this sample was taken inside the Peč cave, and the soil there is influenced by the erosion of limestone rocks and decomposed calcite ending up in the soil. The percentage of hydrogen and nitrogen ranges from 0.58% to 1.74% and from 0.11% to 0.86%, respectively.

At locations S5-S8, a significantly lower carbonate content is observed compared to samples from the Peč cave and Bukovica locations. The cause can be found in the thicker layer of soil present at these locations (S5 and S6), as well as in the fact that Pliocene and Oligocene sedimentation of clastic materials was later eroded by weathering processes from the hypsometrically lower parts of Suva planina Mt., where the sampling locations (S6-S8) were situated. The nitrogen content positively correlates with the organic carbon content, indicating that nitrogen is bound to organic matter, which is present in the soil composition (SMILJKOVIĆ, 2019; PETROVIĆ, 2020b). The total carbon (C) content after carbonate removal ranges from 0.98% to 12.42%. A higher percentage of total carbon (C) in sample S1 is associated with a greater amount of organic matter, indicated not only by the increased organic carbon content but is also visually observed, as these samples had significantly more plant and animal remains. The sulphur content in all samples is below the detection limit, indicating the absence of sulphate and sulphide minerals, as well as the absence of contamination with sulphur organic compounds. The values of organic carbon content (C_{org}) range from 0.38% to 4.92%. It was not possible to determine the organic carbon content in the sediment sample, as it is almost 99.9% carbonate that dissolved during acidic digestion. The main mineral components in the soil samples are aluminosilicate, likely represented by clay minerals, as well as Si, Al, and Fe oxides. An exception in this regard is the S2 sample taken inside the Peč cave, where Ca (in the form of carbonates) dominates, and which is compositionally most like the reference sediment.

Except for S2, of all the macroelements in the soil samples (Fig. 7), silicon is the most abundant, followed by aluminium, indicating that the main mineral component in the samples is aluminosilicates, likely represented by clay minerals. In the soil samples, the concentration of calcium has a wide range (from 3.917 to 149.046 mg/g), which is consistent with the extremely high concentration of carbonates. The concentration of magnesium in the soil samples is 110 times lower than the concentration of Ca in the sediment S9 sample, indicating that the rock sample is almost entirely composed of $CaCO_3$. The concentrations of Mg and Si are similar in sample S9, suggesting that besides carbonates, some Mg may also be present in the form of silicates. The concentration of iron in S9 can be considered significant, although it is only at 345.87 µg/g. All other macro- and microelements in the rock sample have significantly lower contents <300 µg/g.

The concentrations of trace elements: As, Cd, Co, Cr, Cu, Ni, Pb, Se and Zn were compared (Fig. 8) with the permissible metal concentrations in sediments and soil (OFFICIAL GAZETTE RS, 2018). Basic correlations of the analysed elements have also been completed (Supplement 1) (SMILJKOVIĆ, 2019).

The concentration of As is above the permissible value in samples S4-S8, with the concentration in samples S6 and S7 exceeding the remediation values, while it was not detected in the sediment. Arsenic did not show a correlation with any of the macro- and microelements, nor with the content of organic carbon, indicating that it is likely partially present in the organic and partially inorganic components of the soil. The concentration of Cd is above the permissible value in all samples except in sample S6, while it was not detected in sample S9. The concentration of Co is above the permissible value in all samples. Concentrations of Cr were below the permissible concentration for soil in all samples. The concentration of

Figure 8. The concentration of trace elements in the soil samples (S1-S8) and rock sample (S9).

Cu is above the permissible value only in sample S2. Cu has shown a remarkably positive correlation with Ca and a solid one with carbonates (Supplement 1), indicating that it is mainly present in the form of carbonates, i.e. natural basic carbonates such as malachite, $Cu_2(OH)_2CO_3$, and azurite, $Cu_3(OH)_2(CO_3)_2$. Therefore, the elevated concentration of Cu in sample S2 can also be explained by its geogenic origin, as the high concentration of this trace element was observed in the sediment itself, represented by nearly pure carbonate, which was used as a reference sample. The concentration of Ni is above the permissible value in all soil samples except for S2, while in the sediment, it is an order of magnitude lower. Based on the results of the correlation matrix (SMILJKOVIĆ, 2019), a statistically significant positive correlation between Ni content and Fe content, as well as the content of these two elements with Co content, was observed. Considering that these are siderophile elements, the elevated concentration of Ni is most likely of geogenic origin. The concentration of Pb is above the permissible value only in sample S4. The concentration of Se is above the permissible value in all samples but in samples S5 and S8 was not detected. The concentration of Zn is above the permissible value in samples S2 and S4.

The results of soil analyses have shown that there are many trace elements in the composition of the soil, which can enrich the mineral composition of the water infiltrating through the soil on its way to groundwater and yielding at karst springs. Most of them are associated with the presence of clayey (aluminosilicate) particles that constitute the soil. However, analyses of the chemical composition of groundwater from karst springs (Mokra, Divljana, Gornjekoritničko, Bežište) have shown that the content of mineral substances significantly reflects an influence of carbonate rocks through which water percolates and circulates on its way to the point at which groundwater emerges from the aquifer (PETROVIĆ, 2020b). Therefore, the soil together with epikarst (because sometimes the boundary is not visible) can be regarded as a medium for the initial alteration of the quality of infiltrated surface water (usually in the form of rain and melted snow). These alterations are fragmentary, in other words, alterations may start in the soil, and some may occur in the epikarst layer, but the most substantial alteration of karst groundwater quality occurs within the saturated zone of the karst aquifer – limestones (dolostones).

CONCLUSION

The results obtained using satellite imagery (remote sensing) have helped in defining the epikarst at the regional level (eastern slopes of the Suva planina Mt.). The designed E (epikarst potential) map aided in defining the regional development of the epikarst and served as a basis for more detailed mapping of the epikarst during field research as well

as in a better understanding of the area's geology and geomorphology and defining locations of geophysics surveys and rock and soil sampling locations.

Geomorphological field research methods provided a better understanding of the degree of karstification, thus leading to a better definition of the distribution of the epikarst and its characteristics in the eastern slopes of Suva planina Mt.

For defining the characteristics of the epikarst, (hydro) geological mapping was conducted on benchmark profiles defined according to the E map altogether with geomorphological field research. Basic characteristics of the epikarst were defined on site, including the thickness and surface areas on exposed outcrops and sections. Four categories of epikarst were identified. It is advisable to use other remote sensing methods as well, such as the use of unmanned aerial vehicles, especially in parts of the terrain with a particular potential for the formation of epikarst, characterized as inaccessible for visits and on-site measurements.

Geophysical surveys were conducted at four locations, with a total of 15 probes, within the research area using the geoelectric method, employing the vertical electrical sounding (VES) procedure with a Schlumberger-type electrode display. The collected data provided new insights into the thickness and distribution of fractured and karstified zones up to a depth of 30 (100) metres, as well as in defining the thickness of the epikarst in areas subjected to geophysical surveys, thus helping in extrapolation of collected data of single point assessment conducted during mapping.

Petrological/sedimentological research precisely defined the types of limestone rocks at selected locations, each representing one type of carbonate rocks on the eastern slopes of the Suva planina Mt.

Pedological analyses allowed better definition of the soil types based on the macrocomponent content of soil, geochemical characterization of soil and pollution, as well as the definition of organic-geochemical parameters of that, in combination with epikarst, the very first layer which at the same time protects, changes and sometimes could pollute infiltrated water.

Therefore, the soil along with the epikarst (since the boundary is sometimes indistinct) can be considered as a medium for the initial alteration of the quality of infiltrating surface water (typically in the form of rain and melted snow). These alterations are fragmentary, and changes may begin in the soil or occur within the epikarst layer, but the most significant impact on karst groundwater quality takes place in the saturated zone of the karst aquifer.

Research on the eastern slopes of Suva planina Mt. should continue and extend to the entire mountain massif. This comprehensive approach, incorporating multidisciplinary and detailed geological research that comprises geomorphology, geophysics, hydrogeology, sedimentology and pedology, is necessary to understand the catchment area of springs, as well as the circulation patterns of groundwater in this complex hydrogeological system.

Technical constraints during the 2018-2020 field investigations limited the number of vertical electrical sounding surveys, indicating a need for a broader application of this technique in future studies across other locations on Suva planina Mt. Utilizing geoelectric tomography and/or ground-penetrating radar could provide a more comprehensive picture of the epikarst development and the unsaturated zone within the karst aquifer system of Suva planina Mt.

To accurately map the distribution of epikarst on the eastern slopes, an increased density of mapping points is needed. Pre-field drone surveys should be conducted to identify reference profiles in less accessible areas.

Enhancing soil geochemical characterization requires increasing the number of samples from more reference profiles. These profiles should overlap with those used for defining epikarst characteristics. Future soil sampling campaigns should focus on areas with noticeable changes in vegetation type and density.

ACKNOWLEDGEMENT

The authors would like to thank the Ministry of Science, Technological Development and Innovation for providing resources under Contract no. 451-03-66/2024-03/200126 and Contract no. 451-03-65/2024-03/200126. The authors would also like to thank Milena DUNČIĆ, M.Sc., Eng. of geology on the preparation of paleontological analyzes of limestones.

REFERENCES

CHEN, Z., AULER, A.S., BAKALOWICZ, M., DREW, D., GRIGER, F., HARTMANN, J., JIANG, G., MOOSDORF, N., RICHTS, A., STEVANOVIC, Z., VENI, G. & GOLDSCHEIDER, N. (2017): The World Karst Aquifer Mapping project: concept, mapping procedure and map of Europe.– Hydrogeol J, 25, 771-785. https://doi.org/10.1007/s10040-016-1519-3

FLUGEL, E. (2004): Microfacies of Carbonate Rocks: Analysis, Interpretation and Application.– Springer-Verlag, Berlin, Heidelberg, New York, 976 p. http://dx.doi.org/10.1007/978-3-662-08726-8

FOLK, R.L. (1959): Practical petrographic classification of limestones.– Bulletin American Association Petroleum Geologists, 43, 1-38.

GOLDSCHEIDER, N. & DREW, D. (2007): Methods in karst hydrogeology, international contribution to hydrogeology.– Taylor & Francis/Balkema, London, 264 p.

KLIMCHOUK, A.B. (2000): The formation of epikarst and its role in vadose speleogenesis.– In: KLIMCHOUK, A.B., FORD, D.C., PALMER, A.N. & DREYBRODT, W. (eds.): Speleogenesis: Evolution of karst aquifers. National Speleological Society of America, Huntsville, 261-273.

KLIMCHOUK, A.B. (2004): Towards defining, delimiting and classifying epikarst: Its origin, processes and variants of geomorphic evolution, speleogenesis and evolution of karst aquifers.– Speleogenesis and Evolution of Karst Aquifers, 2/1, 1-13.

MARINOVIĆ, V. & PETROVIĆ, B. (2021): Stochastic simulation and prediction of turbidity dynamics in karst systems. Case study: Mokra karst spring (SE Serbia).– Review of the Bulgarian Geological Society, 82/3, 222–224. https://doi.org/10.52215/rev.bgs.2021.82.3.222

OFFICIAL GAZETTE OF THE REPUBLIC OF SERBIA (2018): No. 30/2018: Regulation on limit values of polluting, harmful, and dangerous substances in soil.

PETROVIĆ, B. (2020a): Intrinsic groundwater vulnerability assessment by multiparameter methods, a case study of Suva planina Mountain (SE Serbia).– Environ Earth Sci, 79, 85. https://doi.org/10.1007/s12665-020-8825-8

PETROVIĆ, B. (2020b): The functioning and impact of epikarst oh the regime, balance and groundwater quality of the eastern part of the Suva planina mountain karst system [in Serbian, Abstract in English].– Unpubl. PhD Thesis, University of Belgrade, 305 p.

PETROVIĆ, B. (2023): The Flow Conditions in the Epikarst Zone of a Karst Aquifer. Case Study: Suva planina Mt., East Serbia.– In: International Scientific Conference, Man and Karst 2022, September 12th - 17th, Custonaci, Italy. Ragusa, 123-129.

PETROVIĆ, B. & MARINOVIĆ, V. (2021): Application of the Discrete Autoregressive – Cross-Regressive Moving Average Model for Predicting the Daily Discharge Values of Mokra and Divljana Springs.– Reports of the Serbian geological society year 2020, 1 – 15.

PETROVIĆ, B. & MARINOVIĆ, V. (2023): Quantitative and Geochemical Characterization of the Mokra Karst Aquifer (SE Serbia) by Time Series Analysis and Stochastic Modelling.– In: ANDREO, B., BARBERÁ, J.A., DURÁN-VALSERO, J.J., GIL-MÁRQUEZ, J.M., MUDARRA, M. (eds): EuroKarst 2022, Málaga. Advances in Karst Science. Springer, Cham. https://doi.org/10.1007/978-3-031-16879-6_8

PETROVIĆ, B., STEVANOVIĆ, Z., MARINOVIĆ, V. & IGNJATOVIĆ S. (2022): Prostorna analiza epikarsta u okviru karstnog sistema istočnog dela Suve planina [*Spatial Analysis of Epikarst Within Karst System of Eastern Part of Suva Planina Mountain* – in Serbian].– In: XVI Srpski simpozijum o hidrogeologiji sa međunarodnim učešćem. Univerzitet u Beogradu, Rudarsko-geološki fakultet, Beograd, 365-370.

PETROVIĆ, B., MARINOVIĆ, V. & STEVANOVIĆ, Z. (2023): Characterization of the eastern Suva planina Mt. karst aquifer (SE Serbia) by time series analysis and stochastic modelling.– Environ Earth Sci, 82, 222. https://doi.org/10.1007/s12665-023-10911-5

PETROVIĆ, J. (1976): Jame i pećine SR Srbije [*Jamas and caves of SR Srbija* – in Serbian].– Vojnoizdavački zavod, Beograd, p. 511.

REYNOLDS, J.M. (2011): An Introduction to Applied and Environmental Geophysics, 2nd Edition.– Wiley-Blackwell, 712 p.

SMILJKOVIĆ, Ž. (2019): Geohemijska karakterizacija zemljišta sa istočnih obronaka Specijalnog rezervata prirode „Suva planina“ [*Geochemical characterization of soil from the eastern slopes of the Special Nature Reserve "Suva Planina"* – in Serbian].– Unpubl. Master thesis, University of Belgrade, 47 p.

STEVANOVIĆ, Z. (1991): Hidrogeologija karsta Karpato-Balkanida istočne Srbije i mogućnosti vodosnabdevanja [*Karst hydrogeology of the Carpatho-Balkanides of eastern Serbia and water supply possibilities* – in Serbian].– University of Belgrade, Faculty of Mining and Geology, Belgrade, 245 p.

STEVANOVIĆ, Z. (1994): Karst groundwaters of Carpatho-Balkanides in Eastern Serbia.– In: STEVANOVIĆ Z. & FILIPOVIĆ B. (eds.): Groundwaters in Carbonate Rocks of the Carpatho-Balkan Mountain Range. Carpathian-Balkan Geological Association, Belgrade, 203-237.

STEVANOVIĆ, Z. (2015): Karst Aquifer – Characterization and Engineering.– Springer, 692 p. https://doi.org/10.1007/978-3-319-12850-4

TORRESE, P. (2020): Investigating karst aquifers: Using pseudo 3-D electrical resistivity tomography to identify major karst features.– Journal of Hydrology, 580, 124257. https://doi.org/10.1016/j.jhydrol.2019.124257

VERESS, M., DEAK, G. & MITRE, Z. (2023): The vertical electrical sounding (VES) of the epikarst: a case study of the covered karst of the Bakony region (Hungary).– Acta Carsologica, 52/2-3, 245-258. https://doi.org/10.3986/ac.v52i2-3.12149

VUJISIĆ, T., NAVALA, M., KALENIĆ, M., KRSTIĆ, B., MASLAREVIĆ, LJ., MARKOVIĆ, B., BUKOVIĆ, J. (1971): Osnovna geološka karta SFRJ 1:100.000, Tumač za list Bela Palanka K34-33 [*The Basic Geological Map of SFRY 1:100.000, Explanatory text of the Bela Palanka sheet K34-33* – in Serbian].– Savezni geološki zavod, Beograd, 69 p.

WON-IN, K. & CHARUSIRI, P. (2003): Enhancement of thematic mapper satellite images for geological mapping of the Cho Dien area, Northern Vietnam.– International Journal of Applied Earth Observation and Geoinformation, 4/3, 183-193.

Web sources:

AGRICOLUS (2024): NDVI and NDMI vegetation indices: instructions for use, Available at: https://www.agricolus.com/en/vegetation-indices-ndvi-ndmi/. Accessed: 12/06/24.

ARCGIS (2024): Convolution function, Available at: https://desktop.arcgis.com/en/arcmap/latest/manage-data/raster-and-images/convolution-function.htm. Accessed: 11/06/24.

GISGeography (2024): Landsat 8 Bands and Band Combinations, Available at: https://gisgeography.com/landsat-8-bands-combinations/. Accessed: 21/05/24.

Supplement 1. – Pearson correlation matrix of soil samples analyses.

Corellation		Al	Ca	Fe	K	Mg	Na	Si	As	Cd	Co	Cr	Cu	Li	Mn	Ni	Pb	Se	Sr	Zn	Corg	Carbonates
AL	Pearson correlation	1	-0.697	0.847	0.626	-0.277	0.334	0.659	0.259	0.35	0.63	0.8	-0.492	0.767	0.076	0.869	0.309	-0.7	-0.567	-0.426	-0.06	-0.819
	Sig. (2-tailed)	.	0.037	0.004	0.072	0.47	0.38	0.053	0.502	0.355	0.069	0.01	0.179	0.016	0.847	0.002	0.419	0.08	0.111	0.253	0.878	0.007
	N	9	9	9	9	9	9	9	9	9	9	9	9	9	9	9	9	7	9	9	9	9
Ca	Pearson correlation	-0.697	1	-0.932	-0.544	0.741	-0.517	-0.649	-0.281	-0.213	-0.893	-0.963	0.891	-0.96	-0.033	-0.89	-0.291	0.671	0.919	0.668	-0.078	0.613
	Sig. (2-tailed)	0.037	.	0,000	0.13	0.022	0.154	0.059	0.465	0.581	0.001	0,000	0.001	0,000	0.933	0.001	0.448	0.099	0,000	0.049	0.841	0.079
	N	9	9	9	9	9	9	9	9	9	9	9	9	9	9	9	9	7	9	9	9	9
Fe	Pearson correlation	0.847	-0.932	1	0.752	-0.507	0.58	0.686	0.369	0.166	0.859	0.965	-0.792	0.97	0.091	0.968	0.207	-0.767	-0.793	-0.722	-0.104	-0.816
	Sig. (2-tailed)	0.004	0,000	.	0.019	0.164	0.101	0.041	0.329	0.669	0.003	0,000	0.011	0,000	0.816	0,000	0.593	0.044	0.011	0.028	0.791	0.007
	N	9	9	9	9	9	9	9	9	9	9	9	9	9	9	9	9	7	9	9	9	9
K	Pearson correlation	0.626	-0.544	0.752	1	0.037	0.796	0.571	0.409	-0.347	0.592	0.686	-0.548	0.675	-0.09	0.762	0.046	-0.575	-0.261	-0.668	-0.42	-0.899
	Sig. (2-tailed)	0.072	0.13	0.019	.	0.925	0.01	0.108	0.275	0.361	0.093	0.041	0.127	0.046	0.818	0.017	0.907	0.177	0.498	0.049	0.26	0.001
	N	9	9	9	9	9	9	9	9	9	9	9	9	9	9	9	9	7	9	9	9	9
Mg	Pearson correlation	-0.277	0.741	-0.507	0.037	1	-0.295	-0.497	-0.027	-0.41	-0.736	-0.636	0.617	-0.574	-0.203	-0.396	-0.577	0.142	0.776	0.114	-0.113	-0.023
	Sig. (2-tailed)	0.47	0.022	0.164	0.925	.	0.44	0.174	0.945	0.274	0.024	0.066	0.076	0.106	0.601	0.292	0.104	0.761	0.014	0.771	0.772	0.954
	N	9	9	9	9	9	9	9	9	9	9	9	9	9	9	9	9	7	9	9	9	9
Na	Pearson correlation	0.334	-0.517	0.58	0.796	-0.295	1	0.686	0.224	-0.376	0.731	0.642	-0.55	0.546	-0.011	0.529	0.438	-0.082	-0.207	-0.361	-0.58	-0.529
	Sig. (2-tailed)	0.38	0.154	0.101	0.01	0.44	.	0.041	0.562	0.318	0.025	0.062	0.125	0.128	0.978	0.144	0.238	0.861	0.592	0.34	0.102	0.143
	N	9	9	9	9	9	9	9	9	9	9	9	9	9	9	9	9	7	9	9	9	9
Si	Pearson correlation	0.659	-0.649	0.686	0.571	-0.497	0.686	1	-0.068	0.148	0.851	0.758	-0.385	0.606	0.385	0.645	0.613	-0.418	-0.349	-0.302	-0.535	-0.535
	Sig. (2-tailed)	0.053	0.059	0.041	0.108	0.174	0.041	.	0.863	0.703	0.004	0.018	0.306	0.084	0.307	0.06	0.079	0.351	0.357	0.43	0.138	0.137
	N	9	9	9	9	9	9	9	9	9	9	9	9	9	9	9	9	7	9	9	9	9
As	Pearson correlation	0.259	-0.281	0.369	0.409	-0.027	0.224	-0.068	1	-0.129	0.056	0.226	-0.453	0.306	-0.275	0.292	-0.049	-0.171	-0.338	-0.226	0.151	-0.464
	Sig. (2-tailed)	0.502	0.465	0.329	0.275	0.945	0.562	0.863	.	0.74	0.886	0.558	0.221	0.424	0.473	0.446	0.901	0.714	0.373	0.559	0.698	0.208
	N	9	9	9	9	9	9	9	9	9	9	9	9	9	9	9	9	7	9	9	9	9
Cd	Pearson correlation	0.35	-0.213	0.166	-0.347	-0.41	-0.376	0.148	-0.129	1	0.157	0.175	0.024	0.212	0.337	0.182	0.365	-0.34	-0.38	0.217	0.163	0.18
	Sig. (2-tailed)	0.355	0.581	0.669	0.361	0.274	0.318	0.703	0.74	.	0.687	0.652	0.951	0.585	0.375	0.639	0.334	0.456	0.313	0.576	0.675	0.643
	N	9	9	9	9	9	9	9	9	9	9	9	9	9	9	9	9	7	9	9	9	9
Co	Pearson correlation	0.63	-0.893	0.859	0.592	-0.736	0.731	0.851	0.056	0.157	1	0.93	-0.708	0.855	0.276	0.787	0.484	-0.488	-0.694	-0.517	-0.327	-0.52
	Sig. (2-tailed)	0.069	0.001	0.003	0.093	0.024	0.025	0.004	0.886	0.687	.	0,000	0.033	0.003	0.472	0.012	0.187	0.266	0.038	0.154	0.391	0.151
	N	9	9	9	9	9	9	9	9	9	9	9	9	9	9	9	9	7	9	9	9	9
Cr	Pearson correlation	0.8	-0.963	0.965	0.686	-0.636	0.642	0.758	0.226	0.175	0.93	1	-0.838	0.969	0.032	0.945	0.375	-0.667	-0.806	-0.638	-0.083	-0.719
	Sig. (2-tailed)	0.01	0,000	0,000	0.041	0.066	0.062	0.018	0.558	0.652	0,000	.	0.005	0,000	0.934	0,000	0.32	0.102	0.009	0.064	0.831	0.029
	N	9	9	9	9	9	9	9	9	9	9	9	9	9	9	9	9	7	9	9	9	9
Cu	Pearson correlation	-0.492	0.891	-0.792	-0.548	0.617	-0.55	-0.385	-0.453	0.024	-0.708	-0.838	1	-0.874	0.371	-0.786	-0.216	0.49	0.853	0.632	-0.276	0.56
	Sig. (2-tailed)	0.179	0.001	0.011	0.127	0.076	0.125	0.306	0.221	0.951	0.033	0.005	.	0.002	0.325	0.012	0.576	0.264	0.003	0.068	0.472	0.116
	N	9	9	9	9	9	9	9	9	9	9	9	9	9	9	9	9	7	9	9	9	9
Li	Pearson correlation	0.767	-0.96	0.97	0.675	-0.574	0.546	0.606	0.306	0.212	0.855	0.969	-0.874	1	-0.027	0.965	0.208	-0.754	-0.862	-0.733	0.024	-0.718
	Sig. (2-tailed)	0.016	0,000	0,000	0.046	0.106	0.128	0.084	0.424	0.585	0.003	0,000	0.002	.	0.945	0,000	0.591	0.05	0.003	0.025	0.951	0.029
	N	9	9	9	9	9	9	9	9	9	9	9	9	9	9	9	9	7	9	9	9	9
Mn	Pearson correlation	0.076	-0.033	0.091	-0.09	-0.203	-0.011	0.385	-0.275	0.337	0.276	0.032	0.371	-0.027	1	-0.059	0.049	-0.15	0.039	0.019	-0.626	0.13
	Sig. (2-tailed)	0.847	0.933	0.816	0.818	0.601	0.978	0.37	0.473	0.375	0.472	0.934	0.325	0.945	.	0.88	0.901	0.749	0.921	0.961	0.071	0.74
	N	9	9	9	9	9	9	9	9	9	9	9	9	9	9	9	9	7	9	9	9	9
Ni	Pearson correlation	0.869	-0.89	0.968	0.762	-0.396	0.529	0.645	0.292	0.182	0.787	0.945	-0.786	0.965	-0.059	1	0.179	-0.833	-0.746	-0.74	-0.018	-0.845
	Sig. (2-tailed)	0.002	0.001	0,000	0.017	0.292	0.144	0.06	0.446	0.639	0.012	0,000	0.012	0,000	0.88	.	0.646	0.02	0.021	0.023	0.963	0.004
	N	9	9	9	9	9	9	9	9	9	9	9	9	9	9	9	9	7	9	9	9	9
Pb	Pearson correlation	0.309	-0.291	0.207	0.046	-0.577	0.438	0.613	-0.049	0.365	0.484	0.375	-0.216	0.208	0.049	0.179	1	0.276	-0.174	0.427	-0.236	0.024
	Sig. (2-tailed)	0.419	0.448	0.593	0.907	0.104	0.238	0.079	0.901	0.334	0.187	0.32	0.576	0.591	0.901	0.646	.	0.549	0.655	0.252	0.542	0.952
	N	9	9	9	9	9	9	9	9	9	9	9	9	9	9	9	9	7	9	9	9	9
Se	Pearson correlation	-0.7	0.671	-0.737	-0.575	0.142	-0.082	-0.418	-0.171	-0.34	-0.488	-0.667	0.49	-0.754	-0.15	-0.833	0.276	1	0.603	0.868	-0.094	0.746
	Sig. (2-tailed)	0.08	0.099	0.044	0.177	0.761	0.861	0.351	0.714	0.456	0.266	0.102	0.264	0.05	0.749	0.02	0.549	.	0.152	0.011	0.842	0.054
	N	7	7	7	7	7	7	7	7	7	7	7	7	7	7	7	7	7	7	7	7	7
Sr	Pearson correlation	-0.567	0.919	-0.793	-0.261	0.776	-0.207	-0.349	-0.338	-0.38	-0.694	-0.806	0.853	-0.862	0.039	-0.746	-0.174	0.603	1	0.555	-0.375	0.403
	Sig. (2-tailed)	0.111	0,000	0.011	0.498	0.014	0.592	0.357	0.373	0.313	0.038	0.009	0.003	0.003	0.921	0.021	0.655	0.152	.	0.121	0.319	0.282
	N	9	9	9	9	9	9	9	9	9	9	9	9	9	9	9	9	7	9	9	9	9
Zn	Pearson correlation	-0.426	0.668	-0.722	-0.668	0.114	-0.361	-0.302	-0.226	0.217	-0.517	-0.638	0.632	-0.733	0.019	-0.74	0.427	0.868	0.555	1	-0.014	0.696
	Sig. (2-tailed)	0.253	0.049	0.028	0.049	0.771	0.34	0.43	0.559	0.576	0.154	0.064	0.068	0.025	0.961	0.023	0.252	0.011	0.121	.	0.971	0.037
	N	9	9	9	9	9	9	9	9	9	9	9	9	9	9	9	9	7	9	9	9	9
Corg	Pearson correlation	-0.06	-0.078	-0.104	-0.42	-0.113	-0.58	-0.535	0.151	0.163	-0.327	-0.083	-0.276	0.024	-0.626	-0.018	-0.236	-0.094	-0.375	-0.014	1	0.136
	Sig. (2-tailed)	0.878	0.841	0.791	0.26	0.772	0.102	0.138	0.698	0.675	0.391	0.831	0.472	0.951	0.071	0.963	0.542	0.842	0.319	0.971	.	0.727
	N	9	9	9	9	9	9	9	9	9	9	9	9	9	9	9	9	7	9	9	9	9
Carbonates	Pearson correlation	-0.819	0.613	-0.816	-0.899	-0.023	-0.529	-0.535	-0.464	0.18	-0.52	-0.719	0.56	-0.718	0.13	-0.845	0.024	0.746	0.403	0.696	0.136	1
	Sig. (2-tailed)	0.007	0.079	0.007	0.001	0.954	0.143	0.137	0.208	0.643	0.151	0.029	0.116	0.029	0.74	0.004	0.952	0.054	0.282	0.037	0.727	.
	N	9	9	9	9	9	9	9	9	9	9	9	9	9	9	9	9	7	9	9	9	9